A HYBRID TOTAL-VARIATION MINIMIZATION APPROACH TO COMPRESSED SENSING

Yong Wang[1,2], Dong Liang[2,3], Yuchou Chang[2], Leslie Ying[2]

[1] School of Electronic Engineering, Xidian University, Xi'an, P.R. China
[2] Department of Electrical Engineering and Computer Science, University of Wisconsin-Milwaukee, Milwaukee, WI, USA
[3] Institute of Biomedical and Health Engineering, Shenzhen Institutes of Advanced Technology, Shenzhen, P.R. China

ABSTRACT

Compressed sensing (CS) has been successfully applied to accelerate conventional magnetic resonance imaging (MRI) with Fourier encoding. Total variation (TV) is usually used as the regularization function for image reconstruction. However, it is know that such ℓ_1 - based minimization algorithm needs more measurements than the ℓ_0 -based ones. On the other hand, ℓ_0 -based minimization is computational intractable and unstable. In this paper, we propose a hybrid total variation (HTV) which effectively integrates both ℓ_1 -norm and ℓ_0 -norm of the image gradient by introducing a threshold. The HTV minimization algorithm has the benefits of both the robustness of ℓ_1 and fewer measurements of ℓ_0. Simulations and *in vivo* experiments demonstrate the proposed method outperforms the conventional TV minimization algorithm.

Index Terms— Compressed sensing, magnetic resonance imaging, hybrid total variation, total variation, image reconstruction

1. INTRODUCTION

In recent years, compressed sensing (CS) [1,2] has emerged as a promising signal processing technique that unifies signal sensing and signal compression into a single task. Its basic principle is the use of incoherence measurements to acquire an efficient, dimensionally reduced representation of a sparse signal. With the prior information on sparseness, the original signal can still be recovered from the low-dimensional representation by solving a nonlinear optimization problem.

Specifically, CS considers the problem to reconstruct a signal $\mathbf{x}$ of size n from m linear measurements $\mathbf{y} = \mathbf{\Phi x}$, where $m << n$. Such an underdetermined system entails infinite number of solutions in general. With the prior information that the signal $\mathbf{x}$ is sparse, the sparsest solution should be sought for. Ideally, ℓ_1 is the best metric for sparsity. The signal is recovered by solving a constrained ℓ_0 minimization problem

$$\min_{\mathbf{x}} \|\mathbf{x}\|_0 \quad s.t. \quad \mathbf{\Phi x} = \mathbf{y} \tag{1}$$

where $\|\mathbf{x}\|_0 = \sum_i I_i, \quad I_i = \begin{cases} 1, & x_i \neq 0 \\ 0, & x_i = 0 \end{cases}$.

However, the ℓ_0 minimization problem is computationally intractable and unstable. The most popular surrogate for ℓ_0 is ℓ_1 defined as $\|\mathbf{x}\|_1 = \sum_i |x_i|$. It is primarily because ℓ_1 -norm is convex and the robustness of ℓ_1 minimization is guaranteed [3]. However, more measurements are required for ℓ_1 minimization [4]. Non-convex surrogates have also been investigated [5-8] to reduce measurements of ℓ_1, but usually at the cost of increased computation and/or reduced robustness.

CS has demonstrated success in speeding up magnetic resonance imaging (MRI) via reduced sampling. In MRI, the measurement is made in k-space or the spatial frequency domain. In CS reconstruction, total variation (TV) or ℓ_1 -norm of the image gradient is usually used in the constrained minimization [9, 10]. The TV of an image is defined as

$$\|\mathbf{x}\|_{\mathrm{TV}} = \sum_{i,j} |\nabla x_{i,j}| = \sum_{i,j} \sqrt{\left(D^h_{i,j}x\right)^2 + \left(D^v_{i,j}x\right)^2} \tag{2}$$

where $D^h_{i,j}x$ and $D^v_{i,j}x$ are the horizontal and vertical gradients of the image at location (i, j). TV has the nice property of convex and robustness. However, the required number of k-space samples is large when the image has many details.

In this paper, we propose a new metric, named hybrid TV (HTV) to improve conventional TV in CS reconstruction. It extends our earlier work on hybrid ℓ_0 - ℓ_1 minimization [11]. Specifically, the HTV of the image is defined to be same as TV when the local image gradient is small and a constant otherwise. HTV approximates the ℓ_0 of image gradient, which better promotes sparseness, but improves convergence by use of ℓ_1 in majority of locations across the image. The new metric effectively integrates both ℓ_0 and ℓ_1 and thus has the benefits of both. Simulations and MR experiments demonstrate the proposed HTV

minimization method outperforms the state-of-the-art TV minimization method.

2. PROPOSED HYBRID TOTAL VARIATION

The proposal method minimizes the HTV of the desired image **x** subjected to the data consistent constraint. Without loss of generality, we assume the local gradient $\nabla_{i,j}x$ is bounded by one across the entire image. Mathematically, we solve

$$\min_{\mathbf{x}} \|\mathbf{x}\|_{\mathrm{HTV}} \quad s.t. \quad \mathbf{\Phi x} = \mathbf{y} \tag{3}$$

where $\mathbf{\Phi}$ is the Fourier encoding matrix for reduced sampling, **y** is the undersampled k-space data, and HTV is defined as

$$\| \mathbf{x} \|_{\mathrm{HTV}} = \sum_{i,j} f(\nabla_{i,j}x) \tag{4}$$

where $f(\nabla_{i,j}x) = \begin{cases} |\nabla_{i,j}x|, & |\nabla_{i,j}x| < \tau \\ 1, & |\nabla_{i,j}x| \geq \tau \end{cases}$ and $\tau \leqslant 1$ is a fixed threshold. Fig. 1 illustrates the ideal piecewise function *f* for HTV in contrast to that of TV.

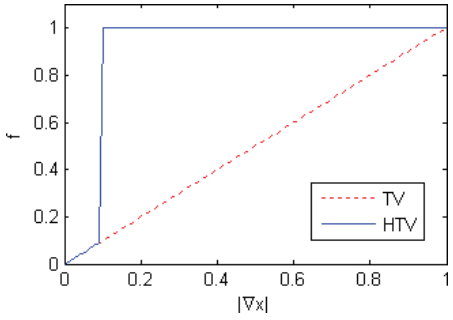


Fig. 1: Plots of the *f* function for TV and HTV (τ=0.1)

It is seen that the proposed HTV includes TV as a special case when τ = 1. As τ approaches zero, HTV becomes the ℓ_0 of the image gradient. For any 0 < τ < 1, HTV mixes ℓ_1 and ℓ_0 depending on the local gradient at individual locations and can be regarded as a hybrid ℓ_1-ℓ_0 of the image gradient. The value of τ controls the contributions from ℓ_1 or ℓ_0 respectively. For large τ, HTV is closer to a convex function and thus has better convergence to the global minimum. On the other hand, for small τ, HTV is computing the sparsity (i.e., number of nonzero elements) of the gradient more accurately without taking into account its actual value. Therefore, an optimal τ would best compromise between these two cases.

In our implementation, we solve the unconstrained optimization problem instead:

$$\min_{\mathbf{x}}(\| \mathbf{y} - \mathbf{\Phi x} \|_2 + \lambda \|\mathbf{x}\|_{\mathrm{HTV}}) \tag{5}$$

where the regularization parameter λ is chosen to balance the contribution of each term. Gradient descent method [12] is used to implement the proposed HTV minimization algorithm. In each iteration, the image at pixel (*i*, *j*) is updated by

$$x_{i,j}^{k+1} = x_{i,j}^{k} - \mu_j^k \nabla_{i,j} H\left(\mathbf{x}^k\right) \tag{6}$$

where *H*(.) is the objective function defined in Eq. (5), *k* denotes the iteration index, and μ is the gradient descent factor. The gradient of the HTV is given as the sum of

$$\nabla_{i,j} \|\mathbf{x}\|_{\mathrm{HTV}} = \begin{cases} \dfrac{D_{i,j}^h x}{|\nabla x_{i,j}|} + \dfrac{D_{i,j}^v x}{|\nabla x_{i,j}|} - \dfrac{D_{i-1,j}^h x}{|\nabla x_{i-1,j}|} - \dfrac{D_{i,j-1}^v x}{|\nabla x_{i,j-1}|}, & |\nabla x_{i,j}| < \tau \\ 0, & |\nabla x_{i,j}| \geq \tau \end{cases} \tag{7}$$

over all pixels, where a small ε is added to the denominator to avoid dividing by zero.

When the same optimization algorithm (e.g. gradient descent here) is used, the computational complexity of the proposed method is about the same as that of TV. However, due to the non-convexity of HTV, an accurate initial guess is desirable for convergence to a high quality image. In our study, we use the TV reconstruction as the initial guess for the image.

3. RESULTS

3.1. Image reconstruction quality

The proposed HTV minimization algorithm was tested on both numerical phantom and an *in vivo* brain dataset. The objective of the phantom study was to evaluate the proposed method in the ideal scenario that the image gradient is perfectly sparse and the measurement is noise free. A 256×256 Shepp-Logan phantom shown in Fig. 2 (a) was used to simulate the k-space data and then randomly undersampled using the variable-density sampling pattern [9] shown in Fig. 2 (b). The sampling rate was 11.5% of the Nyquist rate.

Both the proposed HTV and conventional TV minimization algorithms were used to reconstruct the phantom image from the undersampled k-space data, and the reconstructions are shown in Fig. 2 (c) and (e), respectively. The corresponding error images are shown in Fig. 2 (d) and (f) with 20-time amplification. To make a fair comparison, the same conditions were assumed for both HTV and TV, including the same sampling pattern, optimization algorithm (gradient-based method), and regularization parameter. It is seen that the proposed method is able to reconstruct a high quality image with only 11.5% of sampling, while TV reconstruction is poor at the same sampling rate. The error images show that the reconstruction error of the proposed method is primarily on the edges of the image.

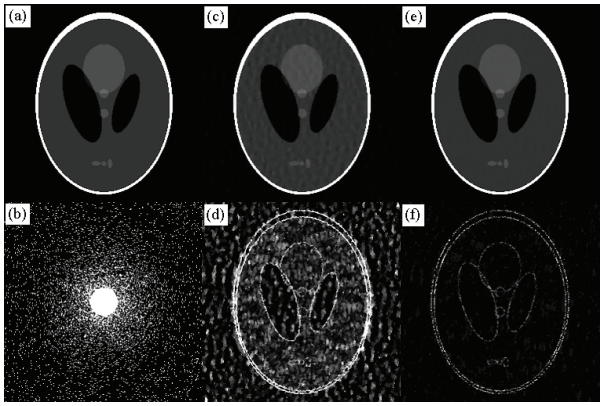


Fig. 2 Comparison of HTV and TV reconstruction using Shepp Logan phantom. (a) Original image; (b) Random sampling pattern in k-space with 11.5% sparse sampling; (c) TV reconstruction and (d) its error image; (e) HTV reconstruction and (f) its error image.

In *in vivo* experiment, the proposed HTV approach was tested on a set of *in vivo* sagittal brain data (see in Fig.3 (a)). The data were acquired using a spin echo (SE) sequence (TR = 500 ms, TE = min full, matrix size = 256 × 256, FOV = 240 mm2). A variable-density random sampling pattern was used to retrospectively undersampling the k-space in both directions with 20% sparse sampling rate. Both the conventional TV and the proposed HTV methods were used to reconstruct the image from the undersampled data. The reconstructions are compared in Fig. 3. TV is seen to fail at such a high reduction factor. The reconstruction has severe blocky artifacts and most details are lost. In contrast, HTV is able to obtain a much cleaner image and preserve more details than TV with the same sampling pattern.

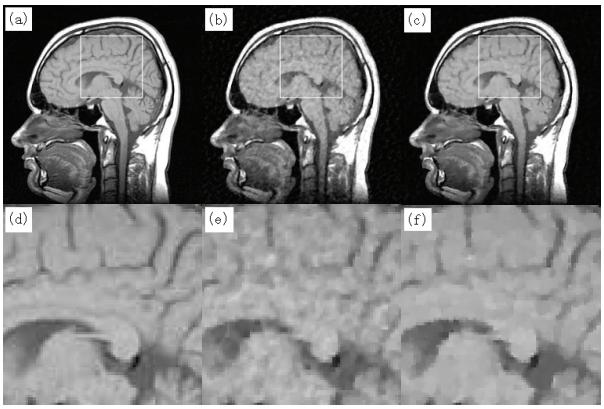


Fig.3 Comparison of HTV and TV reconstruction using vivo brain dataset. (a-c) Original, TV, and HTV (τ=0.1) reconstructions and (d-f) the corresponding zoomed region-of-interest (ROI).

3.2. Effect of sampling rate

We compare the performance of HTV and TV at different sampling rate using the Shepp-Logan phantom. For quantitative comparison, we use the normalized mean-squared error (NMSE), defined as follows:

$$\mathrm{NMSE} = \|\hat{\mathbf{x}} - \mathbf{x}\|_2^2 \big/ \|\mathbf{x}\|_2^2 \qquad (8)$$

where $\hat{\mathbf{x}}$ and $\mathbf{x}$ are the recovered and original images, respectively. For each sampling rate, we randomly generate a sampling pattern and then use HTV and TV to reconstruct the phantom from the same set of sparse samples. The NMSEs of both methods are plotted as a function of the sampling rate in Fig. 4.

It is seen in Fig. 4 that the HTV method has lower NMSEs than TV at low sampling rates (approximately < 14%). The HTV also has better image reconstruction quality than TV. When the sampling rate is high, both methods can reconstruct the image almost exactly. On the other hand, when the sampling is too low (approximately < 10%), the reconstructions of both methods are too poor to be acceptable.

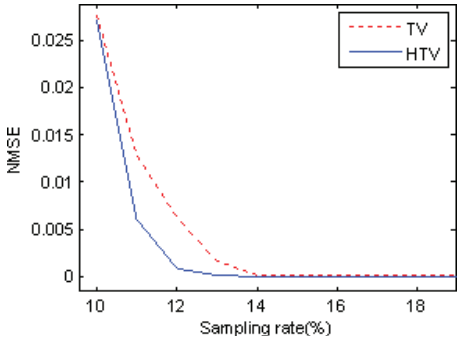


Fig. 4 Comparison of NMSE at different sampling rate

3.3. Effect of threshold

The primary difference of HTV from TV is the introduction of a threshold τ. The choice of τ plays a critical role in the performance of HTV method. To investigate the effect of τ on reconstruction accuracy, we plot the NMSE of the phantom image in Fig. 5 when different τ values are used in HTV reconstruction. A sampling rate of 11.5% was chosen in the experiment. The NMSE of TV is shown as a constant line in the same plot of Fig. 5.

The figure shows that when the threshold gradually increases from 0 to 1, the reconstruction quality of HTV initially improves, then degrades, and eventually approaches that of TV. The reason that HTV is poorer than TV when $\tau \approx 0$ is because the stability of the method is poor when the method approaches ℓ_0 minimization that is a concave problem. When τ is sufficiently large (but still ≤ 1), HTV becomes superior to TV in reconstruction accuracy with $\tau = 0.1$ being the optimal threshold for this particular case. As τ further increases, HTV approaches TV in definition and thus in performance as well. The relatively wide range of τ that HTV outperforms TV suggests that the proposed HTV is practically useful even with a heuristic choice of τ.

Systematic choice of τ is an important topic and will be further studied in future work.

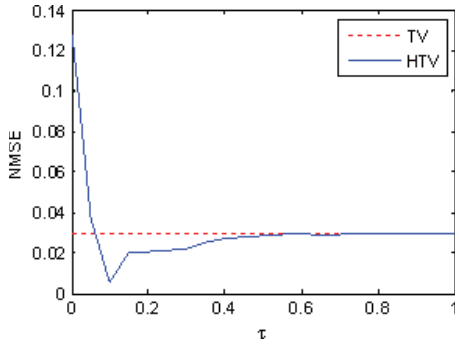


Fig 5 Comparison of NMSEs of TV and HTV with different thresholds

4. DISCUSSION AND CONCLUSION

In this paper, we present a novel compressed sensing MRI reconstruction algorithm based on hybrid total variation. The method has TV reconstruction as a special case when the threshold is set to 1. The proposed approach is shown to outperform TV method using both phantom simulations and *in vivo* experiments. Although we have used the hybrid norm to improve TV here, the same concept can be extended to ℓ_1 -norm of any sparsifying transforms. The algorithm can be used not only in CS MRI reconstruction as demonstrated here, but also in many other applications where compressed sensing is useful.

5. ACKNOWLEDGMENT

This work is supported in part by the Fundamental Research Funds for the Central University (K50511020020，K50511020027), the Research Fund for the Doctoral Program of Higher Education (200807011007), and the Young Backbone Project of China Scholarship to Wang and the US National Science Foundation CBET-0731226 to Ying.

6. REFERENCES

[1] E. J. Candès, J. Romberg and T. Tao, "Robust uncertainty principles: Exact signal reconstruction from highly incomplete frequency information," *IEEE Transaction on Information Theory*, vol. 52, pp. 489-509, Feb. 2006.

[2] D. L. Donoho, "Compressed sensing," *IEEE Transactions on Information Theory*, vol. 52, pp. 1289 - 1306, Apr. 2006.

[3] E. J. Candès, J. Romberg, "Sparsity and incoherence in compressed sampling," *Inverse Problems*, vol. 23, pp. 969-985, Apr. 2007.

[4] E. J. Candès and M. B. Wakin, "An introduction to compressive sampling," *IEEE Signal Processing Magazine*, vol. 25, no. 2, pp. 21-30, Mar. 2008.

[5] J. Trzasko and A. Manduca, "Highly undersampled magnetic resonance image reconstruction via homotopic l0-minimization," *IEEE Transactions on Medical Imaging*, vol.28, no.1, pp.106-121, Jan. 2009.

[6] G. Gasso, A. Rakotomamonjy and S. Canu, "Recovering sparse signals with a certain family of nonconvex penalties and DC programming," *IEEE Transactions on Signal Processing*, vol. 57, no. 12, pp. 4686-4698, Dec. 2009.

[7] R. Chartrand, "Exact Reconstruction of Sparse Signals via Nonconvex Minimization," *IEEE Signal Processing Letters,* vol. 14, no. 10, pp. 707-710, Oct. 2007.

[8] E. J. Candès, M. B. Wakin and S. P. Boyd. "Enhancing Sparsity by Reweighted L1 Minimization," *Journal of Fourier Analysis and Applications*, vol. 14, pp. 877-905, 2008.

[9] M. Lustig, D. Donoho and J. M. Pauly, "Sparse MRI: The application of compressed sensing for rapid MR imaging," *Magnetic Resonance in Medicine*, vol. 58, pp. 1182-1195, Dec. 2007.

[10] B. Liu, K. King, M. Steckner, J. Xie, J. Sheng and L. Ying, "Regularized SENSE reconstruction using Bregman iterations," *Magnetic Resonance in Medicine*, vol. 61, No. 1, pp. 145-152, Jan. 2009.

[11] D. Liang and L. Ying, "A hybrid L_0-L_1 minimization algorithm for compressed sensing MRI," *Proceedings of International Society of Magnetic Resonance in Medicine Scientific Meeting*, 2010.

[12] D. Qi and W. Sha, "The Physics of Compressive Sensing and the Gradient-Based Recovery Algorithms," 2009. http://arxiv.org/abs/0906.1487.